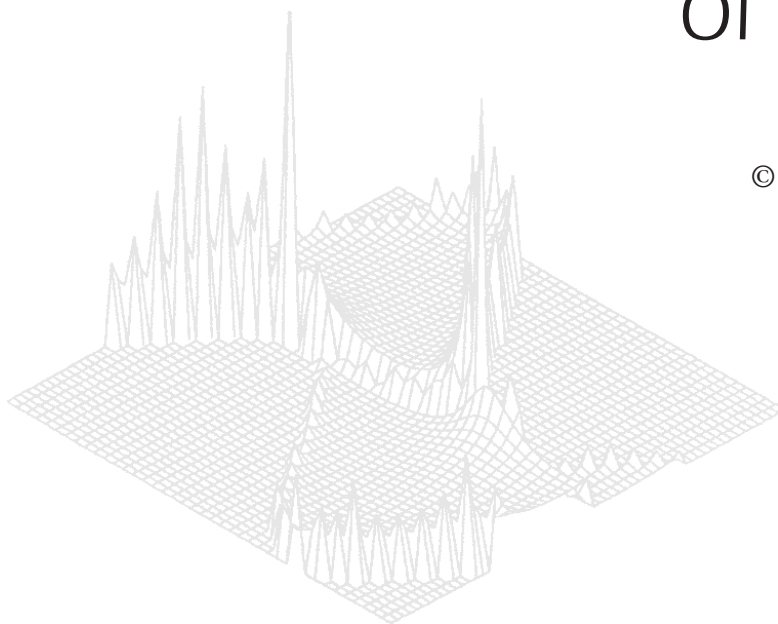

C S I R O P U B L I S H I N G

Australian Journal of Physics

Volume 50, 1997
© CSIRO Australia 1997



A journal for the publication of
original research in all branches of physics

www.publish.csiro.au/journals/ajp

All enquiries and manuscripts should be directed to

Australian Journal of Physics

CSIRO PUBLISHING

PO Box 1139 (150 Oxford St)

Collingwood

Vic. 3066

Australia

Telephone: 61 3 9662 7626

Facsimile: 61 3 9662 7611

Email: peter.robertson@publish.csiro.au



Published by **CSIRO PUBLISHING**
for CSIRO Australia and
the Australian Academy of Science



Tokamak Equilibrium Model with Finite Toroidicity Effects

Jerome L. V. Lewandowski

Department of Theoretical Physics and, Plasma Research Laboratory,
Research School of Physical Sciences and Engineering,
Australian National University, Canberra, ACT 0200, Australia.

Abstract

An inverse aspect ratio ($= \epsilon$) expansion of a low-pressure, axisymmetric tokamak equilibrium is presented. The usual assumption of the $s - \alpha$ model (sharp pressure gradient in a small layer) is used to determine the first order correction in ϵ for various physical quantities. In the infinite aspect ratio limit, the results of the standard $s - \alpha$ model are recovered. Finite toroidicity effects on ion temperature-gradient-driven ballooning modes are discussed and a numerical comparison between the two models is presented.

1. Introduction

There is a general consensus that instabilities with long parallel wavelength but short perpendicular wavelength ($k_{\parallel}/k_{\perp} \ll 1$) are detrimental with respect to the maximum achievable β and to the cross-field transport in magnetic fusion devices. Ideal magnetohydrodynamic (MHD) ballooning modes set a limit to the maximum achievable β . In a toroidal confined plasma, slow drift-type modes, known as drift waves, are believed to be responsible for the anomalous transport observed in tokamaks (Liewer 1985; Tang 1978; Wooton *et al.* 1990; Horton 1989) and in stellarators (Boozer *et al.* 1990; Wagner and Stroth 1993).

For modes with $k_{\parallel}/k_{\perp} \ll 1$, a Wentzel–Kramers–Brillouin (WKB) representation simplifies the formulation of stability problems. For low-pressure axisymmetric plasmas the detail of the confining magnetic field assumes a simple form known as the $s - \alpha$ model (Cooner *et al.* 1978), where s is the global magnetic shear and α is a measure of the pressure gradient. In the infinite aspect ratio limit, s and α enter the equilibrium as two independent parameters. Inclusion of finite toroidicity effects imposes a maximum allowable pressure gradient (for a given ϵ). The $s - \alpha$ model is widely used in calculations of MHD ballooning modes (Jarmen *et al.* 1987; Anderson and Weiland 1986, 1988; Rewoldt *et al.* 1987; Hirose *et al.* 1994, 1995), drift-type modes (Shukla *et al.* 1990; Connor and Taylor 1987; Hirose and Elia 1996; Taylor *et al.* 1996; Hastie *et al.* 1979; Sen and Weiland 1995) and resistive ballooning modes (Novakosvskii *et al.* 1995; Terry and Diamond 1985).

In this paper, we consider an ideal tokamak configuration with shifted magnetic surfaces. A systematic expansion in terms of the inverse aspect ratio is presented.

The usual assumption of the standard $s - \alpha$ model, i.e. sharp pressure gradient in a narrow layer, is used to simplify the final expressions. It is shown that the radial derivative of the Shafranov shift enters the equilibrium on an equal footing with first-order toroidicity effects. We illustrate the difference between the two models by considering the high- n ballooning mode equation in tokamak geometry.

2. High- n Ballooning Modes

The high- n ballooning modes, at marginal stability ($\omega^2 = 0$), are described by the following (Coppi 1977; Dobrott *et al.* 1977; Connor *et al.* 1978):

$$\nabla_{\parallel} \left(|\nabla \alpha_f|^2 \nabla_{\parallel} \hat{\Phi} \right) + \frac{2}{B |\nabla \psi|} \frac{dp}{d\psi} \left(\kappa_N + \kappa_G \frac{I}{B^2} |\nabla \psi|^2 \right) \hat{\Phi} = 0, \quad (1)$$

where $\hat{\Phi}$ is the ballooning eigenfunction, ∇_{\parallel} is the parallel gradient operator keeping the field line label α_f constant, ψ is the enclosed poloidal flux and p is the equilibrium plasma pressure. Further, κ_N and κ_G are, respectively, the normal and geodesic components of the magnetic curvature $\kappa \equiv \hat{\mathbf{e}}_{\parallel} \cdot \nabla \hat{\mathbf{e}}_{\parallel}$ where $\hat{\mathbf{e}}_{\parallel} \equiv \mathbf{B}/B$ is a unit vector parallel to the equilibrium magnetic field \mathbf{B} . In equation (1)

$$\begin{aligned} I &\equiv - \frac{\nabla \alpha_f \cdot \nabla \psi}{|\nabla \psi|^2} \\ &= \frac{\hat{\mathbf{n}}}{|\nabla \psi|} \cdot \nabla \left(\int_{\theta_0}^{\theta} Q d\theta \right) \end{aligned} \quad (2)$$

is the so-called integrated local shear, where $Q \equiv \mathbf{B} \cdot \nabla \zeta / \mathbf{B} \cdot \nabla \theta$ is the local pitch of the magnetic field lines, $\hat{\mathbf{n}} \equiv \nabla \psi / |\nabla \psi|$ is a unit vector normal to the magnetic surface $\psi = \text{const.}$, θ and ζ are the poloidal and toroidal angle-like coordinates with period 2π , respectively, and θ_0 is the poloidal angle at which the integration along the field line is started. The first term on the left-hand side of equation (1) contains the *stabilising* contribution of the field line bending. The term proportional to the pressure gradient is the *driving* term responsible for the mode to ‘balloon’ in the region of unfavourable magnetic curvature (that is where κ_N is negative). The ballooning drive also contains the effect of the geodesic component of the magnetic curvature coupled to the integrated local shear.

The parallel gradient operator, keeping the field line label α_f constant, can be written as

$$\nabla_{\parallel} = \frac{\xi_{\parallel}(\theta)}{qR_0} \frac{\partial}{\partial \theta}, \quad (3)$$

where R_0 is the magnetic axis radius, q is the safety factor and $\xi_{||}$ is a nondimensional function, defined along the field line, of the order of unity (see next section). Introducing the modified ballooning function

$$\widehat{\Psi} \equiv \sqrt{f}\widehat{\Phi}, \quad (4)$$

the high- n ballooning equation (1) can be written as

$$\frac{d^2\widehat{\Psi}}{d\theta^2} = Q_{\text{eff}}(\theta)\widehat{\Psi}, \quad (5)$$

where

$$Q_{\text{eff}}(\theta) \equiv \frac{g(\theta)}{f(\theta)} - \frac{1}{4f^2} \left(\frac{df}{d\theta} \right)^2 + \frac{1}{2f} \frac{d^2f}{d\theta^2} \quad (6)$$

is the ‘effective potential’. In equations (4) and (6) we have introduced the following nondimensional quantities

$$f(\theta) \equiv \xi_{||} R_0^2 |\nabla\alpha_f|^2, \quad (7)$$

which represents the stabilising contribution and

$$g(\theta) \equiv -\frac{2q^2 R_0^4}{\xi_{||} B} \frac{dp/d\psi}{|\nabla\psi|} \left(\kappa_N + \kappa_G \frac{I}{B^2} |\nabla\psi|^2 \right) \quad (8)$$

is the ballooning drive. For a nonvanishing global magnetic shear, $s \neq 0$, and for large values of the extended poloidal angle, $|\theta| \gg 1$, the first term on the right-hand side of equation (6) scales like $\sim 1/|\theta|$ whereas the second and third terms, arising from the transformation (4), scale like $\sim 1/|\theta|^2$.

3. The Equilibrium

For analytical and numerical applications, it is customary to represent the confining magnetic field in straight-field-line coordinates (SFLC). Equilibrium magnetic surfaces are assumed to consist of a family of nested torii. The magnetic field lies in the surface of constant pressure $\mathbf{B} \cdot \nabla p \equiv 0$. Under this assumption, the confining magnetic field field can be written in Clebsch form (Dewar and Glasser 1983; Dewar *et al.* 1984; D’haeseleer *et al.* 1983)

$$\mathbf{B} = \nabla\alpha_f \times \nabla\psi, \quad (9)$$

where $2\pi\psi$ is the enclosed poloidal (magnetic) flux and $\alpha_f \equiv \zeta - q(\psi)\bar{\theta}$ is the field line label. Here, $\bar{\theta}$ and ζ are the poloidal and toroidal angle-like variables with period 2π , respectively, while $q(\psi)$ is the safety factor. For equilibria with toroidal symmetry the azimuthal angle ϕ is an ignorable coordinate. Without

loss of generality the toroidal angle can be written as (Greene 1983; White and Chance 1984; White 1989):

$$\zeta = \phi - \lambda(\psi, \bar{\theta}) , \quad (10)$$

showing that ζ is also an ignorable coordinate. Here λ is the so-called stream function. Clearly there are two degrees of freedom in the representation of the magnetic field through the stream function $\lambda(\psi, \bar{\theta})$. One degree of freedom is eliminated by choosing the Jacobian of the transformation of the form $\mathcal{J} \equiv [\nabla\psi \cdot (\nabla\bar{\theta} \times \nabla\zeta)]^{-1} = F(\psi)/B^2$. This particular choice for the Jacobian is due to Grad (1971) and was later investigated by Boozer (1980, 1981, 1982). Plasma equilibria in axisymmetric systems, such as the ideal tokamak configuration, are governed by the Grad–Shafranov equation (Shafranov 1958, 1963, 1966; Ware and Haas 1966; Lust and Schluter 1957; Greene *et al.* 1971):

$$\nabla \cdot \frac{\nabla\psi}{R^2 q} + q \frac{dp}{d\psi} + \frac{Gq}{R^2} \frac{dG}{d\psi} = 0 , \quad (11)$$

where $2\pi G(\psi)$ is the poloidal current flowing outside the flux surface and R is the distance from the axis of revolution to a point on a magnetic surface. The Grad–Shafranov equation (11) is a second-order elliptic partial differential equation and, in general, has to be solved numerically with appropriate conditions at the plasma boundary. However, in the low- β limit equation (11) can be solved by direct expansion in powers of the inverse aspect ratio $\epsilon \equiv a/R_0$, where a is the minor radius of the plasma and R_0 is the magnetic axis radius. For a very-low- β plasma, $\beta \sim \epsilon^3$, and the plasma has a negligible effect on the shape of the magnetic surfaces. To lowest order in ϵ , the equilibrium magnetic surfaces consist of a family of nested, concentric circles (Shafranov 1966*a*). For a low- β plasma, $\beta \sim \epsilon^2$, and the equilibrium magnetic surfaces remain circular but are shifted towards the plasma outboard ($\theta \approx 0$) (Shafranov 1966*b*). The amount of displacement is the so-called Shafranov shift. For a high- β plasma, $\beta \sim \epsilon$, and the magnetic surfaces have elliptical and triangular distortions. In this paper we consider a low- β (ideal) tokamak equilibrium and we assume that the conditions

$$\beta = \mathcal{O}(\epsilon^2) \text{ and } q = \mathcal{O}(1) \quad (12)$$

are satisfied. A safety factor of order unity implies that the poloidal component of the magnetic field is one order smaller in ϵ than its toroidal component. For convenience, the solution to the Grad–Shafranov equation is carried out in the cylindrical coordinate system (R, Z, ϕ) , right-handed in that order, where Z is the vertical axis. A point on a magnetic surface $\psi = \text{const.}$ is specified as follows (White 1989):

$$\begin{aligned} R(r, \theta) &= R_0 + r \cos \theta - \Delta(r) , \\ Z(r, \theta) &= r \sin \theta , \\ \phi &= \phi , \end{aligned} \quad (13)$$

where r is the minor radius measured from the magnetic axis, θ is the local poloidal angle and $\Delta(r)$ is the Shafranov shift. The Shafranov shift vanishes at the magnetic axis ($= R_0$), $\Delta(0) = 0$. In the remainder of this paper we will use the following normalised quantities: $R \rightarrow R/R_0$, $Z \rightarrow Z/R_0$, $r \rightarrow r/R_0$, $\Delta \rightarrow \Delta/R_0$, $p(r) \rightarrow p(r)/B_0^2$ and $B \rightarrow B/B_0$. Here B_0 is the magnetic field strength at the magnetic axis. In these normalised units, we note the following ordering:

$$\begin{aligned} R &\sim q(r) \sim \ddot{\Delta} = \mathcal{O}(1) , \\ r &\sim Z \sim \dot{\Delta} = \mathcal{O}(\epsilon) , \\ p(r) &\sim \beta \sim \Delta(r) = \mathcal{O}(\epsilon^2) , \end{aligned} \quad (14)$$

where a dot denotes a derivative with respect to r . For a low- β equilibrium, the enclosed poloidal flux, written in normalised units,

$$\psi(r) = \int \frac{r}{q(r)} dr , \quad (15)$$

only depends on the local minor radius (White 1989). Therefore r , $q(r)$, $\psi(r)$, or any combination of these quantities, can be alternatively used as appropriate radial labels. Using equation (13) we compute the covariant basis vectors $\mathbf{e}_r \equiv \partial \mathbf{r} / \partial r$, $\mathbf{e}_\theta \equiv \partial \mathbf{r} / \partial \theta$ and $\mathbf{e}_\phi \equiv \partial \mathbf{r} / \partial \phi$, where $\mathbf{r} = R(r, \theta) \hat{\mathbf{R}} + Z(r, \theta) \hat{\mathbf{Z}}$ is the local position vector written in cylindrical coordinates. The Jacobian of the transformation is then easily derived as $\mathcal{J} = (d\psi/dr)^{-1} \mathbf{e}_r \cdot (\mathbf{e}_\theta \times \mathbf{e}_\phi)$. Finally, the contravariant basis vectors are calculated using the relation $\nabla_i \equiv \epsilon_{ijk} \mathcal{J}^{-1} \mathbf{e}_j \times \mathbf{e}_k$ for $\{i, j, k\} = (r, \theta, \phi)$.

Here ϵ_{ijk} is the usual Levi-Civita symbol for permutations. Substituting all these quantities into the Grad–Shafranov equation and expanding to second order in ϵ , equation (11) decouples into a radial and a poloidal part. The radial equation provides an equation for the Shafranov shift (Shafranov 1963, 1966a, 1966b; White 1989):

$$\Delta(r) = \int_0^r \left\{ \frac{q^2}{r'^3} \int_0^{r'} \frac{r''^3}{q^2} \left(1 - 2 \frac{q^2}{r''} \frac{dp}{dr''} \right) dr'' \right\} dr' . \quad (16)$$

For given pressure and safety factor profiles the Shafranov shift is uniquely determined. The θ -dependent part of the Grad–Shafranov shift is used to derive the condition for the magnetic field line to be straight. This yields to a partial differential equation for the stream function (White 1989):

$$\frac{\partial \lambda}{\partial \theta} = \frac{q \bar{\eta}}{R} \left(1 - \frac{R}{\bar{\eta}} \right) , \quad (17)$$

where we have introduced $\bar{\eta}(r, \theta) \equiv 1 - \dot{\Delta} \cos \theta$ and, as before, a dot denotes

a derivative with respect to r . Integrating equation (17) with respect to the poloidal angle we get the field line label

$$\alpha_f = \phi - q\theta + q \{ r + \dot{\Delta} [\sin \theta - \sin \theta_0] \}, \quad (18)$$

where θ_0 denotes the poloidal angle at which the integration along the field line is started. The last term in equation (18) is one order smaller in ϵ than the first two terms.

4. Finite Toroidicity Effects

In this section we derive the functions $f(\theta)$ and $g(\theta)$ entering the ‘effective potential’ Q_{eff} defined by equation (6). Unlike previous studies finite toroidicity effects (corrections of order $\sim \epsilon$) are retained in this paper. As can be seen from the ordering (14) finite ϵ corrections enter on an equal footing with the radial derivative of the Shafranov shift.

The lowest-order WKB wavevector assumes the form $\mathbf{k}_\perp = m\nabla\alpha_f$, where m is the large mode number. It follows that $\mathbf{k}_\perp \cdot \mathbf{k}_\perp / k_\theta^2 = r^2 \nabla\alpha_f \cdot \nabla\alpha_f / q^2$. Here $k_\theta \equiv mq/r$ is the characteristic perpendicular wavevector. For a second order equilibrium the contravariant basis vectors are (White 1989):

$$\begin{aligned} \nabla r &= \frac{\cos \theta}{\bar{\eta}} \hat{\mathbf{R}} + \frac{\sin \theta}{\bar{\eta}} \hat{\mathbf{Z}}, \\ \nabla \theta &= -\frac{\sin \theta}{r\bar{\eta}} \hat{\mathbf{R}} + \frac{\cos \theta - \dot{\Delta}}{r\bar{\eta}} \hat{\mathbf{Z}}, \\ \nabla \phi &= \frac{\hat{\phi}}{R}, \end{aligned} \quad (19)$$

where $(\hat{\mathbf{R}}, \hat{\mathbf{Z}}, \hat{\phi})$ are unit cylindrical vectors. The nonorthogonality of the coordinate system arises from the $\dot{\Delta}$ contribution in equation (19).

Straightforward algebra yields

$$\begin{aligned} \frac{\mathbf{k}_\perp \cdot \mathbf{k}_\perp}{k_\theta^2} &= \frac{1}{\bar{\eta}^2} \left\{ \left(\frac{r\bar{\eta}}{qR} \right)^2 + A^2 - 2 \dot{\Delta} \sin \theta A [(r + \dot{\Delta}) \cos \theta - 1] \right. \\ &\quad \left. + [1 - 2 \dot{\Delta} \cos \theta + \dot{\Delta}^2] [(r + \dot{\Delta}) \cos \theta - 1]^2 \right\}, \end{aligned} \quad (20)$$

where

$$A \equiv \alpha_0 (\sin \theta - \sin \theta_0) - s\theta \quad (21)$$

contains the secular behaviour of $\nabla\alpha_f$ and $s \equiv rdq/dr/q$ is the global magnetic shear parameter. We have introduced the ‘generalised’ ballooning parameter

$$\alpha_0 \equiv \frac{r}{q} \frac{d}{dr} \left[q \left(r + \dot{\Delta} \right) \right]. \quad (22)$$

Equation (20) contains all orders in the inverse aspect ratio ϵ . Expanding (20) in ascending powers of ϵ , and taking into account the ordering (14), we get:

$$\begin{aligned} \frac{\mathbf{k}_\perp \cdot \mathbf{k}_\perp}{k_\theta^2} &= (1 + A^2) \left(1 + 2 \dot{\Delta} \cos \theta \right) + 2 \dot{\Delta} \sin \theta A \\ &\quad - 2 \left(r + 2\dot{\Delta} \right) \cos \theta, \end{aligned} \quad (23)$$

where corrections of order ϵ^2 and higher have been neglected. We now make the usual assumptions used in the standard $s - \alpha$ model (Connor *et al.* 1978). Namely, the pressure gradient is assumed to be large, $\dot{p} = \mathcal{O}(1)$, in a small annulus $\Delta r \sim \epsilon^2$ centred around $r = r_0$. Using equation (16) the radial derivative of the Shafranov shift then becomes

$$\begin{aligned} \dot{\Delta} &\simeq \epsilon - 2 \frac{q^2}{r^3} \int_{r_0 - \Delta r/2}^{r_0 + \Delta r/2} r'^2 \frac{dp}{dr'} dr' \\ &\simeq \epsilon - 2q^2 \dot{p} \epsilon \\ &= (1 + \alpha) \epsilon, \end{aligned} \quad (24)$$

where $\alpha \equiv -2q^2 dp/dr = \mathcal{O}(1)$ is the standard ballooning parameter (i.e. a measure of the pressure gradient). To leading order the second-order radial derivative of the Shafranov shift becomes $\ddot{\Delta} = \alpha/r + \mathcal{O}(1)$, which is the approximation usually used in the standard $s - \alpha$ model. Assuming $r \sim r_0 \sim \epsilon$ (i.e. close to the plasma edge where the normal curvature is unfavourable) the generalised ballooning parameter (22) becomes

$$\alpha_0 = \alpha + \epsilon \left[2 + s + 3(1 + \alpha)(s - 1) \right]. \quad (25)$$

The generalised ballooning parameter depends on α and s . The standard $s - \alpha$ model neglects finite toroidicity effects; in this case the generalised ballooning parameter (25) reduces to the standard ballooning parameter, $\alpha_0 = \alpha$. Using (24) in equation (23) we finally get

$$\begin{aligned} \frac{\mathbf{k}_\perp \cdot \mathbf{k}_\perp}{k_\theta^2} &= (1 + A^2) \left[1 + 2 \epsilon (1 + \alpha) \cos \theta \right] \\ &\quad + 2 \epsilon \left[A(1 + \alpha) \sin \theta - (3 + 2\alpha) \cos \theta \right] + \mathcal{O}(\epsilon^2). \end{aligned} \quad (26)$$

In the infinite aspect ratio limit, $\epsilon \mapsto 0$, equation (26) simplifies drastically. In this case the magnitude of the perpendicular wavevector (for $\theta_0 = 0$) assumes its usual form:

$$k_{\perp} = k_{\theta} \left[1 + (\alpha \sin \theta - s\theta)^2 \right]^{\frac{1}{2}}. \quad (27)$$

The driving term $g(\theta)$ in the effective potential involves the normal and geodesic components of the magnetic curvature. For a flat current profile, the (normalised) magnetic field reads

$$\mathbf{B} = \nabla\phi \times \nabla\psi + Q\nabla\psi \times \nabla\theta, \quad (28)$$

where the first term on the right-hand side corresponds to the poloidal component of the magnetic field, whereas the second term represents the toroidal component of \mathbf{B} . Here $Q \equiv q\bar{\eta}/R$ is the local pitch of the magnetic field lines. For a flat current profile it follows that $B_{\theta} = r/qR\bar{\eta}$ and $B_{\phi} = 1/R$, and the magnetic field can now be written as $\mathbf{B} = B_{\theta}\hat{\theta} + B_{\phi}\hat{\phi}$, where we have defined $\hat{\theta} \equiv \cos\theta \hat{\mathbf{Z}} - \sin\theta \hat{\mathbf{R}}$. Using these forms for B_{θ} and B_{ϕ} , the magnetic curvature can be written as

$$\kappa = \left(b_{\theta}\hat{\theta} \cdot \nabla + b_{\phi}\hat{\phi} \cdot \nabla \right) \left(b_{\theta}\hat{\theta} + b_{\phi}\hat{\phi} \right), \quad (29)$$

where $b_{\theta} \equiv B_{\theta}/B = \mathcal{O}(\epsilon)$ and $b_{\phi} \equiv B_{\phi}/B = \mathcal{O}(1)$. The unit vector normal to the magnetic surface is

$$\hat{\mathbf{n}} \equiv \frac{\nabla\psi}{(\nabla\psi \cdot \nabla\psi)^{\frac{1}{2}}} = \cos\theta \hat{\mathbf{R}} + \sin\theta \hat{\mathbf{Z}}, \quad (30)$$

whereas the unit geodesic vector is $\hat{\mathbf{b}} \equiv \mathbf{B} \times \hat{\mathbf{n}}/B = b_{\phi}\hat{\theta} - b_{\theta}\hat{\phi}$. Using these expressions for $\hat{\mathbf{n}}$ and $\hat{\mathbf{b}}$ and noting that $\hat{\theta} \cdot \nabla\theta = 1/r$, $\hat{\phi} \cdot \nabla\phi = 1/R$ and $\hat{\theta} \cdot \nabla\phi = \hat{\phi} \cdot \nabla\theta = 0$, we get the normal curvature

$$\kappa_{\text{N}} = -\cos\theta + r \left(\cos^2\theta - \frac{1}{q^2} \right) + \mathcal{O}(\epsilon^2) \quad (31)$$

and the geodesic curvature

$$\kappa_{\text{G}} = \sin\theta - r \sin\theta \cos\theta + \mathcal{O}(\epsilon^2). \quad (32)$$

It is worth noting that the Shafranov shift (and its derivatives) only enters in the second-order corrections. The term $-r/q^2$ is the (unfavourable) surface-averaged normal curvature. The parallel gradient operator, keeping the field line label constant, reads

$$\nabla_{\parallel} = \frac{\mathbf{B} \cdot \nabla\theta}{B} \frac{\partial}{\partial\theta}. \quad (33)$$

In physical units, we have

$$\nabla_{\parallel} = \frac{\xi_{\parallel}}{qR_0} \frac{\partial}{\partial \theta}, \quad (34)$$

where

$$\xi_{\parallel} = \frac{1}{\bar{\eta}} = 1 + \dot{\Delta} \cos \theta + \mathcal{O}(\epsilon^2). \quad (35)$$

In the cylindrical limit, $\xi_{\parallel} = 1$, the parallel gradient operator assumes its usual form, $\nabla_{\parallel} = \frac{1}{qR_0} \frac{\partial}{\partial \theta}$. It is worth noting that finite β corrections enter (34) through $\dot{\Delta}$ which, in turn, is of the same order as the toroidicity corrections, $\sim \epsilon$. Using equations (31) and (32) the stabilising contribution in the effective potential reads

$$f(\theta) = \frac{q^2}{r^2} \left\{ 1 + A^2 + \epsilon \left[3(1 + \alpha)(1 + A^2) \cos \theta + 2(1 + \alpha)A \cos \theta - 2(3 + 2\alpha) \cos \theta \right] \right\}, \quad (36)$$

whereas the destabilising contribution is

$$g(\theta) = -\frac{\alpha q^2}{r^2} \left\{ \cos \theta + A \sin \theta + \epsilon \left[A \sin \theta \cos \theta + \frac{1}{q^2} + (1 + \alpha)(1 - 3\cos^2 \theta) \right] \right\}. \quad (37)$$

In the cylindrical limit, $\epsilon \mapsto 0$, we recover the equation of Connor *et al.* (1978). Inclusion of finite toroidicity effects are (1) the appearance of new secular terms (linear and quadratic in A); (2) the strong dependence on the pressure gradient; and (3) the inclusion of higher order harmonics arising from the equilibrium. One can expect substantial modifications in the $s - \alpha$ stability diagram for ballooning modes (Connor *et al.* 1978) and other micro-instabilities such as the ion-temperature-gradient driven (ITG) ballooning modes (Hirose *et al.* 1995). It is indeed the case.

5. Numerical Results and Discussion

The effective potential for high- n ballooning modes as a function of the extended poloidal angle is shown in Fig. 1. The parameters are $s = 0.15$ and $\alpha = 1.0$. In order to minimise the effect of unfavourable normal curvature we have chosen a large value for the safety factor, $q = 3$. In Fig. 1, the dot-dash curve corresponds to the standard $s - \alpha$ model case ($\epsilon = 0$). The solid curve corresponds to the modified model, with $\epsilon = 0.05$. The effective potential at $\theta = \pm\pi$ is smaller when the modified model is used. More importantly, the

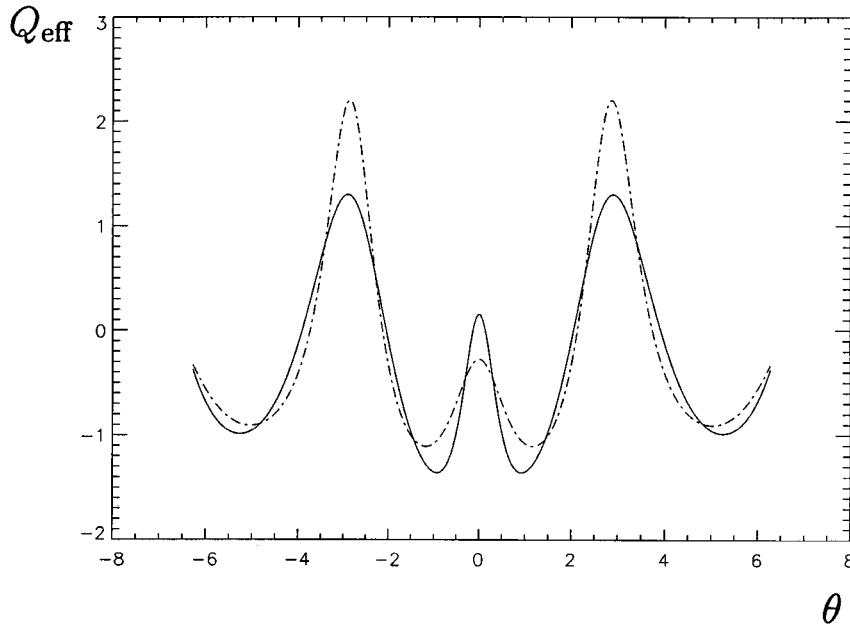


Fig. 1. Effective potential as a function of the extended poloidal angle for the standard $s - \alpha$ model (dot-dash curve) and for the modified $s - \alpha$ model with $\epsilon = 0.05$ (solid curve).

‘hill’ around $\theta = 0$, where the magnetic curvature is unfavourable, is higher and narrower in the modified model than in the standard model. Furthermore, at $\theta = 0$, Q_{eff} is positive in the modified model but negative in the standard model.

In order to access the importance of these modifications, we calculate the field-line-averaged value

$$\langle Q_{\text{eff}}(r) \rangle \equiv \frac{1}{2\theta_c} \int_{-\theta_c}^{+\theta_c} Q_{\text{eff}}(r, \theta') d\theta', \quad (38)$$

where θ_c is determined from the root equation

$$Q_{\text{eff}}(\theta_c) = 0. \quad (39)$$

For $\theta_0 = 0$, the equilibrium is symmetric so that $Q_{\text{eff}}(-\theta_c) = Q_{\text{eff}}(+\theta_c) = 0$. As we previously pointed out in Section 2, the first term in the effective potential, g/f , scales like $\sim 1/|\theta|$ for $|\theta| \gg 1$, whereas the remaining terms scale like $\sim 1/\theta^2$. For a small global shear, the mode will be fairly extended along the field line and the root equation (39) then reduces to

$$g(\theta_c) \simeq 0. \quad (40)$$

Therefore, in the small global shear limit, $g(\theta)$ is destabilising when $|\theta/\theta_c|$ is less than unity but stabilising otherwise. It is now well-known that ballooning modes

can be driven unstable in the region where the normal curvature is destabilising *and* where the local magnetic shear is small (Greene and Chance 1981). In a low-pressure tokamak plasma, the local magnetic shear, written in normalised units, is (Lewandowski and Persson 1995, 1996)

$$\mathcal{S} = s - r \cos \theta \left[1 + \ddot{\Delta} + \frac{\dot{\Delta}}{r} (1 - 2s) \right] + \mathcal{O}(\epsilon^2) . \quad (41)$$

Using the usual assumption of the standard $s-\alpha$ model, $\dot{\Delta} = \mathcal{O}(\epsilon) \ll \ddot{\Delta} = \mathcal{O}(\epsilon^{-1})$, we get

$$\mathcal{S} = s - \alpha \cos \theta + \mathcal{O}(\epsilon) . \quad (42)$$

The second term on the right-hand side is sometimes referred to as the ‘local shear’ (White 1989). It is worth noting that the finite- β corrections in the (driving) normal curvature enter to second order in ϵ . However, finite- β corrections in the (stabilising) local magnetic shear enter to *first* order in ϵ .

When the pressure gradient is small, the local magnetic shear (42) reduces to the global shear s . When the global shear is small, the mode extent along the field line is large and it experiences the favourable effect of toroidal corrections of the normal curvature ($r \cos^2 \theta$ term in equation 31). In the strong shear case, the mode extent along θ is small and it experiences only a small fraction of the region of unfavourable magnetic curvature. In both the above cases, the modes are in the so-called first stability region (Connor *et al.* 1978).

As the pressure gradient increases, the local magnetic shear decreases and ultimately vanishes when $\theta = \cos^{-1}(s/\alpha)$; the mode is driven unstable. For larger pressure gradients, the poloidal field on the outer side of the torus strengthens

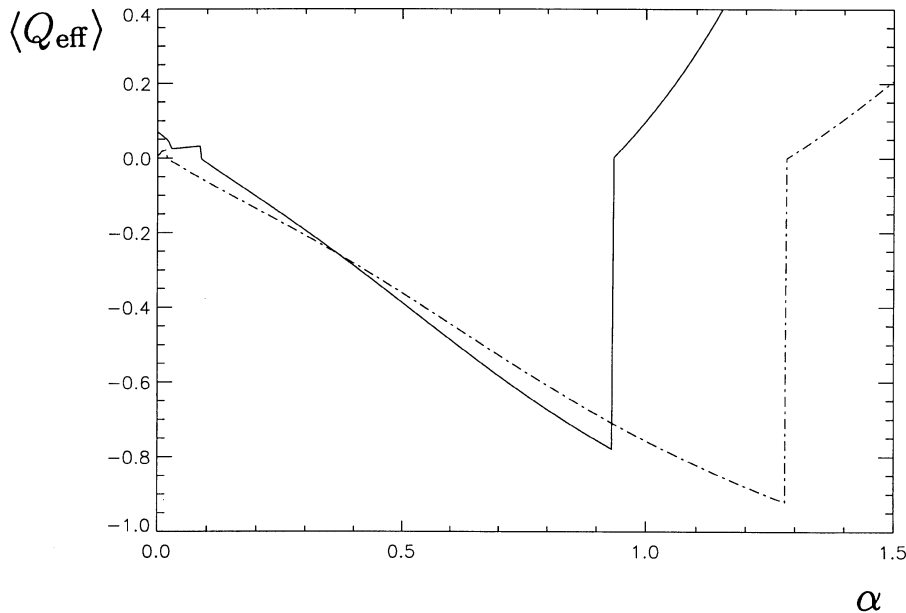


Fig. 2. Field-line-averaged effective potential as a function of the ballooning parameter α for the standard $s-\alpha$ model (dot-dash curve) and for the modified $s-\alpha$ model (solid curve).

and the Shafranov shift increases. This shortens the connection length and, consequently, diminishes the instability drive. This is the second stability region (Connor *et al.* 1978; White 1989).

Since the first-order corrections to the local magnetic shear are important and since the radial derivative of the Shafranov shift enters on an equal footing with toroidal corrections, it is worth studying the modifications to the accessibility to the second stability region. The field-line-averaged effective potential (38) as a function of the pressure gradient parameter α is shown in Fig. 2. The global shear is $s = 0.15$. The transition from negative $\langle Q_{\text{eff}} \rangle$ to positive $\langle Q_{\text{eff}} \rangle$ indicates the approximate position of the second stability region. The dot-dash curve in Fig. 2 corresponds to the standard $s - \alpha$ model ($\epsilon = 0$). The pressure gradient threshold is $\alpha \simeq 1.3$. The solid curve corresponds to the modified $s - \alpha$ model with $\epsilon = 0.05$. The pressure gradient threshold is substantially reduced, $\alpha \simeq 0.92$. The difference in the α threshold between the two models can be understood by close inspection of equations (7) and (8). For $|\theta| \gg 1$, the first-order correction in the stabilising field line bending term (7) scales like $\sim (s\theta)^2$. The driving term (8), however, scales like $\sim s\theta$. Therefore the stabilising contribution varies faster than its driving counterpart, resulting in a lower pressure gradient threshold.

Although not apparent, finite toroidicity corrections in the MHD equilibrium model imposes a limit on the maximum allowable pressure gradient. The parallel gradient operator

$$\nabla_{\parallel} = \frac{1}{qR_0(1 - \Delta \cos \theta)} \frac{\partial}{\partial \theta} \quad (43)$$

must be well-behaved. Recalling (24) the pressure gradient must be chosen so that the condition $\alpha \ll \alpha_c$ occurs where

$$\alpha_c \equiv \frac{1 - \epsilon}{\epsilon} \quad (44)$$

is satisfied. In the cylindrical limit the critical pressure gradient is readily infinite so that α can be chosen arbitrarily large (see for instance Hirose *et al.* 1995). When toroidicity effects are retained in the model, $\epsilon \neq 0$, the maximum allowable α is given by equation (44).

It has been recently suggested that the second stability region for ITG ballooning modes does not exist. Hirose *et al.* (1995) presented this unexpected conclusion using the standard $s - \alpha$ model. A numerical study of ITG ballooning modes in toroidal geometry is presently being carried out. A comparison between the standard and modified $s - \alpha$ models will be reported in a separate paper. Preliminary results indicate that the disappearance of the second stability region for ITG ballooning modes is an *artefact* of the (rather crude) $s - \alpha$ model.

Acknowledgments

The author was supported by a Canadian NSERC research grant and by an Australian National University research grant. Numerical calculations were carried out on the Supercomputer VPP300 at the Australian National University Supercomputer Facility.

References

- Andersson, P., and Weiland, J. (1986). *Phys. Fluids* **29**, 1744.
- Andersson, P., and Weiland, J. (1988). *Phys. Fluids* **31**, 359.
- Boozer, A. H. (1980). *Phys. Fluids* **23**, 904.
- Boozer, A. H. (1981). *Phys. Fluids* **24**, 1999.
- Boozer, A. H. (1982). *Phys. Fluids* **25**, 520.
- Boozer, A. H., Baldwin, D. E., Horton, C. W., Dominguez, R. R., Glasser, A. H., Krommes, J. A., Neilson, G. H., Shaing, K.-C., Sadowski, W. L., and Weitzner, H. (1990). *Phys. Fluids B* **2**, 2870.
- Connor, J. W., and Taylor, J. B. (1987). *Phys. Fluids* **30**, 3180.
- Connor, J. W., Hastie, R. J., and Taylor, J. B. (1978). *Phys. Rev. Lett.* **40**, 396.
- Coppi, B. (1977). *Phys. Rev. Lett.* **39**, 939.
- Dewar, R. L., and Glasser, A. H. (1983). *Phys. Fluids* **26**, 3038.
- Dewar, R. L., Monticello, D. A., and Sy, W. N.-C. (1984). *Phys. Fluids* **27**, 1723.
- D'haeseleer, W. D., Hitchon, W. N. G., Callen, J. D., and Shohet, J. L. (1983). 'Flux Coordinates and Magnetic Field Structure' (Springer: Berlin).
- Dobrott, D., Nelson, D. B., Greene, J. M., Glasser, A. H., Chance, M. S., and Frieman, E. A. (1977). *Phys. Rev. Lett.* **39**, 943.
- Grad, H. (1971). In 'Plasma Physics and Controlled Nuclear Fusion Research', Vol. 3, p. 229 (IAEA: Vienna).
- Greene, J. M. (1983). *Commun. Pure Applied Math.* **36**, 537.
- Greene, J. M., and Chance, M. S. (1981). *Nucl. Fusion* **21**, 453.
- Greene, J. M., Johson, J. L., and Weimer, K. E. (1971). *Phys. Fluids* **14**, 671.
- Hastie, R. J., Kesketh, K. W., and Taylor, J. B. (1979). *Nucl. Fusion* **19**, 1223.
- Hirose, A., and Elia, M. (1996). *Plasma Phys. Contr. Fusion* **38**, 265.
- Hirose, A., Zhang, L., and Elia, M. (1994). *Phys. Rev. Lett.* **72**, 3993.
- Hirose, A., Zhang, L., and Elia, M. (1995). *Phys. Plasmas* **2**, 859.
- Horton, W. (1989). *Phys. Fluids B* **1**, 524.
- Jarmen, A., Andersson, P., and Weiland, J. (1987). *Nucl. Fusion* **27**, 941.
- Lewandowski, J. L. V., and Persson, M. (1995). *Plasma Phys. Contr. Fusion* **37**, 1199.
- Lewandowski, J. L. V., and Persson, M. (1996). *Aust. J. Phys.* **49**, 1121.
- Liewer, P. C. (1985). *Nucl. Fusion* **25**, 543.
- Lust, R., and Schluter, A. (1957). *Z. Naturforsch.* A **12**, 850.
- Novakovskii, S. V., Guzdar, P. N., Drake, J. F., Liu, C. S., and Waelbroeck, E. L. (1995). *Phys. Plasmas* **2**, 781.
- Rewoldt, G., Tang, W. M., and Hastie, R. J. (1987). *Phys. Fluids* **30**, 807.
- Sen, S., and Weiland, J. (1995). *Phys. Plasmas* **2**, 777.
- Shafranov, V. D. (1958). *Sov. Phys. JETP* **6**, 545.
- Shafranov, V. D. (1963). *J. Nucl. Energy C* **5**, 251.
- Shafranov, V. D. (1966a). In 'Reviews of Plasma Physics', Vol. 2 (Consultants Bureau: New York).
- Shafranov, V. D. (1966b). In 'Reviews of Plasma Physics', Vol. 4 (Consultants Bureau: New York).
- Shukla, P. K., Murtaza, G., and Weiland, J. (1990). *J. Plasma Phys.* **44**, 393.
- Tang, W. M. (1978). *Nucl. Fusion* **18**, 1089.
- Taylor, J. B., Wilson, H. R., and Connor, J. W. (1996). *Plasma Phys. Contr. Fusion* **38**, 243.
- Terry, P. W., and Diamond, P. H. (1985). *Phys. Fluids* **28**, 1419.
- Wagner, F., and Stroth, U. (1993). *Plasma Phys. Contr. Fusion* **35**, 1321.
- Ware, A. A., and Haas, F. A. (1966). *Phys. Fluids* **9**, 956.
- White, R. B. (1989). 'Theory of Tokamak Plasmas', Frontiers in Physics (North Holland: Amsterdam).
- White, R. B., and Chance, M. S. (1984). *Phys. Fluids* **27**, 2455.
- Wooton, A. J., Carreras, B. A., Matsumoto, H., McGuire, K., Peebles, W. A., Ritz, Ch. P., Terry, P. W., and Sweben, S. J. (1990). *Phys. Fluids B* **2**, 2879.